

## The Impact of Doppler Lidar Wind Observations on a Single-Level Meteorological Analysis

L. P. RIISHØJGAARD AND R. ATLAS

*Data Assimilation Office, NASA Goddard Space Flight Center, Greenbelt, Maryland*

G. D. EMMITT

*Simpson Weather Associates, Inc., Charlottesville, Virginia*

(Manuscript received 9 June 2003, in final form 31 October 2003)

### ABSTRACT

Through the use of observation operators, modern data assimilation systems have the capability to ingest observations of quantities that are not themselves model variables but are mathematically related to those variables. An example of this is the so-called line-of-sight (LOS) winds that a spaceborne Doppler wind lidar (DWL) instrument would provide. The model or data assimilation system ideally would need information about both components of the horizontal wind vectors, whereas the observations in this case would provide only the projection of the wind vector onto a given direction. The estimated or analyzed value is then calculated essentially as a weighted average of the observation itself and the model-simulated value of the observed quantity. To assess the expected impact of a DWL, it is important to examine the extent to which a meteorological analysis can be constrained by the LOS winds. The answer to this question depends on the fundamental character of the atmospheric flow fields that are analyzed, but, just as important, it also depends on the real and assumed error covariance characteristics of these fields. A single-level wind analysis system designed to explore these issues has been built at the NASA Data Assimilation Office. In this system, simulated wind observations can be evaluated in terms of their impact on the analysis quality under various assumptions about their spatial distribution and error characteristics and about the error covariance of the background fields. The basic design of the system and experimental results obtained with it are presented. The experiments were designed to illustrate how such a system may be used in the instrument concept definition phase.

### 1. Introduction

Despite tremendous progress in numerical weather prediction (NWP) and analysis systems over the last several decades, operational weather forecasts still occasionally go seriously wrong. At a workshop sponsored by the World Meteorological Organization on the impact of observations on NWP (World Meteorological Organization 2000), the lack of independent knowledge about the wind profile in the free troposphere over the oceans was cited as the single most important cause of sporadic, abnormally large forecast errors in the Northern Hemisphere extratropics.

Whereas radiosondes provide adequate wind profile observations over the densely populated land area of the Northern Hemisphere, much of the information about the wind profile over the oceans comes from the multivariate assimilations of satellite temperature soundings (e.g., Lönnberg and Hollingsworth 1986), in

which temperature observations are used to derive information about the atmospheric flow under certain assumptions about the nature of the prevailing balance. An additional important source of information is the set of wind observations calculated by tracking features in the cloud and water vapor images obtained by the geostationary satellites (e.g., Velden et al. 1997; Menzel 2001).

However, both of these sources of information are incomplete. The flow information embedded in the temperature field is indirect, and it is only used correctly when the balance of the real atmosphere corresponds to what is assumed in the analysis system. The geostationary wind data are of a less indirect nature, but for the current generation of satellites the observations are intrinsically single-level or vertically averaged winds, coverage is limited to areas where features can be detected and tracked, the motion of the selected features may not always correctly reflect the mean flow field in their area, and the correct assignment of altitude level to the derived winds remains problematic. Very little useful information about the flow beyond 60° latitude in either hemisphere can be obtained from geostationary

---

*Corresponding author address:* L. P. Riishøjgaard, Data Assimilation Office, NASA Goddard Space Flight Center, Greenbelt, MD 20771.  
E-mail: larspr@gmao.gsfc.nasa.gov

orbit, and current scan practices severely limit the amount of available information beyond 40°S. Note that assimilation of feature-tracked winds using imagery from the Moderate-Resolution Imaging Spectroradiometer (MODIS) instrument has shown promising results in initial tests (e.g., Riishøjgaard and Zhu 2002).

Direct measurement of winds away from the areas of relatively good radiosonde coverage therefore remains a high priority for the global observing system. Such observations are expected to be especially valuable in situations in which the balance assumptions used for assimilation of satellite sounding data are invalid and in regions where the geostationary wind observations are either poor or missing altogether. A spaceborne Doppler wind lidar (DWL) is one of the candidate systems for providing these data. The measurement principle is based on the fact that the Doppler shift of the return from an emitted pulse of monochromatic electromagnetic radiation can be translated into information about the radial velocity of the air at the origin of the return. Only the velocity component aligned with the lidar beam is measured, and the observations are therefore often referred to as line-of-sight (LOS) winds. A DWL instrument can provide a direct wind measurement with an accurate height assignment, and it can provide a relatively uniform horizontal coverage. Several concepts for such wind instruments have been studied in the past (Emmitt 1987; European Space Agency 1999; Gentry et al. 1998), and the European Space Agency has selected the Atmospheric Dynamics Mission (ADM) as one of its two Earth Explorer Core Missions, for a projected 2006 launch.

Both the ADM and some of the concepts studied earlier are single-perspective instruments; that is, the orientation of the LOS with respect to the flight direction of the spacecraft is fixed. The observations therefore consist of a series of projections of the local horizontal wind vector onto essentially parallel lines, which eliminates the need for a scanning mechanism and simplifies the instrument design. Because raw LOS winds have little direct value for the user, the main target application for these observations is data assimilation for numerical weather prediction purposes. The underlying assumption is that the data assimilation system will be able to correctly infer the unobserved wind component orthogonal to the instrument LOS from a combination of the observations themselves, the background field, and the assumed error statistics of the background field.

The purpose of this article is to examine this assumption, along with a few important trade issues that need to be addressed in the definition phase for such an instrument. This examination is done through a series of analysis experiments based on simulated observations obtained from simple, idealized random observation networks. The word analysis is used here in its commonly accepted NWP sense to indicate both the process of blending observational data into a model-estimated field and the result of such a process. The analysis sys-

tem used for the experiments, although simple, captures some of the essential features of a full-scale meteorological analysis system for wind observations. We emphasize here that the goal is not to propose an alternative to the established methodology of observing system simulation experiments (OSSEs; e.g., Atlas 1997) for quantifying the expected impact of a new observation type. Instead, the goal here is to present a simple and versatile framework in which a much broader range of issues can be studied than is possible in the more complete but computationally much more expensive OSSE framework.

Before any experiments can be meaningfully interpreted, a metric of success (or information content) for the different wind observation configurations needs to be defined. Because the target application for these particular observations is data assimilation, we have chosen to use the analysis error variance as the main metric. In other words, the criterion for success of a given observing system configuration is the extent to which it contributes toward producing an analysis with a low expected error. Issues such as measurement error and density of horizontal coverage are considered irrelevant by themselves and are important only insofar as they contribute to achieving this goal.

In the following section, the experimental setup will be reviewed. Next, a series of analysis experiments will be presented. The main issues addressed are 1) the performance of one versus two DWL perspectives, 2) separate versus spatially collocated dual perspectives, and 3) the dependency of the analysis error on the angle between the two perspectives. All of these experiments are carried out with a highly idealized background error covariance model. Based on a fourth set of experiments, the implications of using a more realistic error covariance model are discussed. The fifth and final set of experiments addresses the trade-off between horizontal coverage/resolution on the one hand and measurement accuracy on the other.

## 2. The experimental setup

To explore some of the basic configuration issues for a spaceborne DWL, a simple analysis system for simulated wind observations was developed at the National Aeronautics and Space Administration Data Assimilation Office (DAO). The system takes user-specified “truth” and background states as input, simulates a set of observations of the true state with the required coverage and error characteristics, and produces a wind analysis based on the background and the simulated observations as output.

The analysis equation and the background error covariance models are both similar to what is used in the DAO’s operational Physical-Space Statistical Analysis System (PSAS; Cohn et al. 1998). The most important differences with respect to the full data assimilation system are that 1) the DWL analysis domain consists of a

limited area on a single level, 2) only wind observations are analyzed, and 3) the system does not include a forecast model. The system is easy and inexpensive to set up and run, and it is therefore very well suited to test how observations with different coverage and error characteristics propagate through the analysis equation and, ultimately, how successful they are in reducing the analysis error.

As in most modern meteorological analysis systems (e.g., Lorenc 1986), the analyzed state  $\mathbf{w}^a$  is found by solving the Kalman filter analysis equation

$$\mathbf{w}^a = \mathbf{w}^b + \mathbf{K}(\mathbf{w}^o - \mathbf{H}\mathbf{w}^b). \quad (1)$$

In this equation,  $\mathbf{w}^b$  is the prior, or background state (in an operational context generally coming from a short-range forecast),  $\mathbf{K}$  is the gain matrix,  $\mathbf{w}^o$  is the vector of the observations, and  $\mathbf{H}$  is the observation operator that translates information from the background state into a vector of simulated observations. For  $n$  state variables and  $p$  observations, both  $\mathbf{w}^a$  and  $\mathbf{w}^b$  are  $n$  vectors,  $\mathbf{w}^o$  is a  $p$  vector, and  $\mathbf{H}$  is a  $p \times n$  matrix. The optimal gain matrix, in the sense that the resulting analysis has the smallest expected error, is given by

$$\mathbf{K} = \mathbf{P}^b \mathbf{H}^T (\mathbf{H} \mathbf{P}^b \mathbf{H}^T + \mathbf{R})^{-1}, \quad (2)$$

where  $\mathbf{P}^b$  is the background error covariance matrix and  $\mathbf{R}$  is the observation error covariance matrix. From Eqs. (1) and (2) it is evident that the analysis depends not only on the background field and the observations but also on the assumed error covariance characteristics of the observations and of the background. In rough terms, the diagonal elements of the background and observation error covariance matrices determine the relative weights assigned to the background and observations in the analysis, whereas the off-diagonal elements of the background error covariance matrix in particular define the impact of the observations on the analysis at the unobserved locations and on the unobserved variables.

The length of the state vector for a typical global meteorological forecast model is currently on the order of  $10^7$ . The background error covariance matrix  $\mathbf{P}^b$  nominally contains  $n^2/2$ , that is, on the order of  $10^{14}$ , elements. Because there is no known way of reliably specifying this many independent parameters describing the error statistics for a given forecast system, this matrix is normally modeled using crude assumptions. It is important to keep in mind that any conclusions regarding the impact of a given type of observation on an analysis system will depend critically on the assumptions used in modeling the covariance matrix of that system.

Generally, the univariate background error covariance  $P_{ij}^b$  between the values of a given state variable at two different locations with indices  $i$  and  $j$  is given by

$$P_{ij}^b = \sigma_i \sigma_j \rho_{ij}, \quad (3)$$

where  $\sigma_i$  is the background error standard deviation at point  $i$ , and  $\rho_{ij}$  is the background error correlation be-

tween points  $i$  and  $j$ . In actual implementations, this is often simplified by assuming, for example, that the forecast error correlations only depend on the distance between  $i$  and  $j$  and that the forecast error standard deviations are constant on a given vertical level.

Because the wind is a vector quantity rather than a scalar, the problem of specifying background error covariances for winds is slightly more complicated. Without regard for the vertical component of the wind, it involves specifying the covariances for a set of two scalars as well as the possible cross covariances between them. The two scalars could be orthogonal wind components, or vorticity and divergence, or velocity potential and streamfunction. However, the actual choice of scalars and the functional form of the covariance can both have a profound impact on the quality of the wind analysis. This is particularly evident in the case of incomplete observations, such as wind measurements taken along parallel lines of sight. Here, all of the observational information pertains to one of the two scalars involved, and any information added to the analyzed state about the wind component orthogonal to the observed direction, therefore, comes entirely from the assumptions built into the forecast error covariance matrix.

The assumption of nondivergence, which is frequently used in atmospheric modeling and analysis, can be used to illustrate this last point. Assume that both the truth and the background states are nondivergent. Also, the background error will then be nondivergent. Now, let the two-dimensional wind field  $\mathbf{u} = (u, v)$  be defined in terms of a streamfunction  $\psi$  with a known error covariance matrix  $\mathbf{P}_\psi^b$  through the following relationship:

$$\mathbf{u} = \mathbf{k} \times \nabla \psi, \quad (4)$$

where  $\mathbf{k}$  is the unit vector in the vertical direction.

For discretized numerical applications, it is convenient to express this in operator form:

$$\mathbf{u} = \mathbf{A} \psi, \quad (5)$$

where

$$\mathbf{A} = \begin{bmatrix} -\frac{\partial \psi}{\partial y} \\ \frac{\partial \psi}{\partial x} \end{bmatrix}. \quad (6)$$

Using this operator, the wind error covariance matrix  $\mathbf{P}_u^b$  is easily obtained from the streamfunction error covariance:

$$\mathbf{P}_u^b = \mathbf{A} \mathbf{P}_\psi^b \mathbf{A}^T, \quad (7)$$

where  $\mathbf{A}^T$  is the transpose of  $\mathbf{A}$ . The matrix  $\mathbf{P}_u^b$  will, in general, be full; that is, there will be terms in it that link the error of one wind component to the error of the other. Thus, even if observations of, say, the  $u$  component are provided, the analysis system would still update both the  $u$  and  $v$  components based on the as-

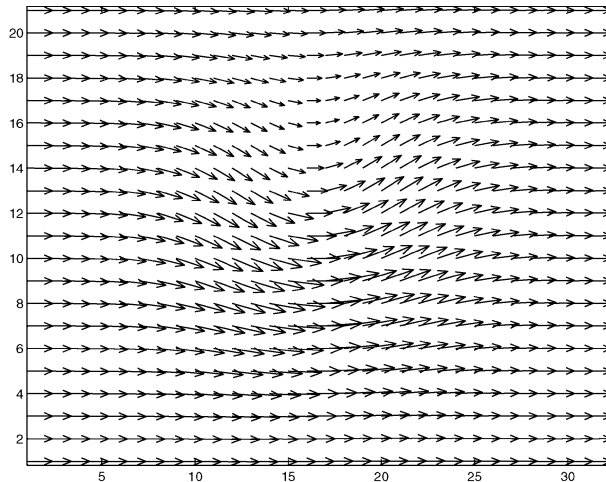


FIG. 1. Vector winds plotted for the true state on a  $31 \times 21$  grid with 100-km grid spacing.

sumption of nondivergence that links the two errors. One might even expect observations of just a single wind component to contain enough information to effectively constrain the analysis in such a case, because the assumption of nondivergence reduces the number of degrees of freedom per grid point from two to one. However, it is easy to see from Eq. (4) that even full knowledge of one wind component mathematically only allows determination of the other component to within a constant of integration. The first set of experiments discussed in the next section was set up to test whether this theoretical limitation can be expected to pose real problems for the single-perspective observations.

### 3. Experimental results

For the experiments described in this section, the true state  $w'$  is a nondivergent zonal flow with a single eddy, as shown in Fig. 1. The analysis domain is a rectangular array of regularly spaced grid points defined at a single vertical level—31 in the zonal direction by 21 in the meridional direction. The grid spacing is fixed at 100 km. The extent of the domain is thus  $2000 \text{ km} \times 3000 \text{ km}$ , and the dimension of the state vector is 1302 ( $31 \times 21 \times 2$ ).

The background state is a zonal flow with a constant velocity over the domain (not shown), and thus the experiments essentially test the ability of the analysis to extract correctly the information from the observations about the presence of a wave in the flow and add it to the background state. This is equivalent to the early detection from real observations of a developing wave that was not present in the short-term forecast, a frequently occurring situation in operational meteorological analysis. The rms difference between the true and background states is  $2.4 \text{ m s}^{-1}$  in both the zonal and meridional wind component. Because both the true state and the background are nondivergent, the background

error will be nondivergent in this framework. Real background errors, on the other hand, are combinations of divergent and nondivergent errors, and the relative amounts in which the two types of errors are present in a given situation is generally unknown. The controlled framework of the experiments presented here has the advantage that the error is known, and the error covariance can therefore be specified correctly (i.e., consistent with the actual background error) or incorrectly (e.g., reflecting typical assumptions made in operational practice about the nature of the background error) as desired.

#### a. One versus two perspectives

In the first series of experiments, the impact on the analysis of having one versus two perspectives of the flow at a given location is explored. The observations consist of samples of the true field at a set of locations that are randomly scattered over the domain. A simulated observation error in the form of uncorrelated Gaussian mean-zero noise with a standard deviation of  $1.0 \text{ m s}^{-1}$  is added to the samples. The number of observations  $p$  is set by the experimenter. For the one-perspective experiments, the samples are  $p$  projections of the true field onto a randomly oriented line of sight. For the initial set of two-perspective experiments, the samples are  $p/2$  projections onto both this and the orthogonal direction. The two types of experiments thus contain the same amount of information, in the sense that the observational dataset contains the same number of scalar values. The purpose of the experiments is to examine whether they also contain the same amount of information in an analysis error reduction sense.

The background error is assumed to be nondivergent and the background wind error covariance matrix is therefore derived from a streamfunction error covariance matrix using Eq. (7). As already mentioned, the assumption of nondivergence is expected to be useful for constraining the unobserved wind component orthogonal to the LOS. The disadvantage of using this assumption is that it excludes any potentially important divergent flows from the analysis. This component of the flow typically contains smaller scales, and it is difficult, at best, to diagnose it from the wind observations that are currently available operationally. Some analysis systems exclude nondivergent flows from the analysis increments altogether outside the tropical regions. The problems that arise from doing this may become more pronounced as the resolution of the models and, hence, the analyses progresses to smaller horizontal scales.

We emphasize again that, although the assumption of nondivergence is correct for this particular experiment, the amount of nondivergence in any given actual atmospheric situation is unknown. The background error covariance formulation used here, however, allows and, in fact, requires the user to specify explicitly the relative amounts of information about the rotational and diver-



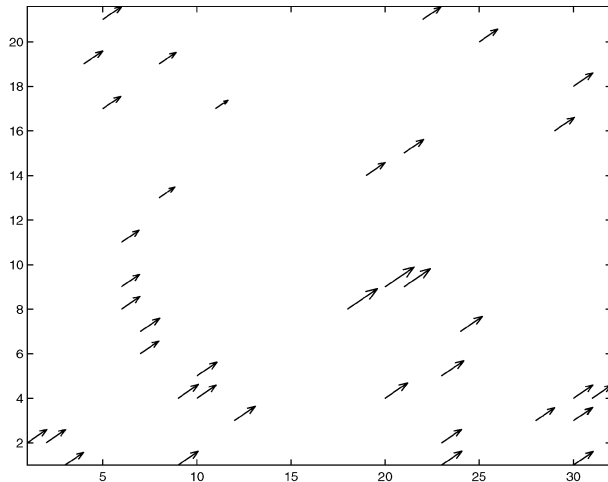


FIG. 2. An example of randomly distributed single LOS observations of the wind state as shown in Fig. 1.

gent components of the flow that should be extracted from the observations.

In Fig. 2, a random set of single-perspective observations is shown for  $p = 40$ , and an LOS azimuth angle of  $60^\circ$ . Although the pattern of samples is atypical of proposed DWL concepts, the random data voids can be thought of as areas of cloud obscurations.

An analysis obtained from the observations in Fig. 2 is shown in Fig. 3. When comparing Figs. 3 and 1, it is evident that, despite the highly favorable specification of the background error, the analysis is only marginally capable of detecting the presence of the eddy from the observations. The analyzed structure lacks intensity, and nonzero  $v$  components are evident throughout the meridional range of the plot.

The rms differences for  $u$  and  $v$  between the true and analyzed states (Figs. 1 and 3) are  $1.3$  and  $1.7 \text{ m s}^{-1}$ , respectively. As one would expect, the error reduction

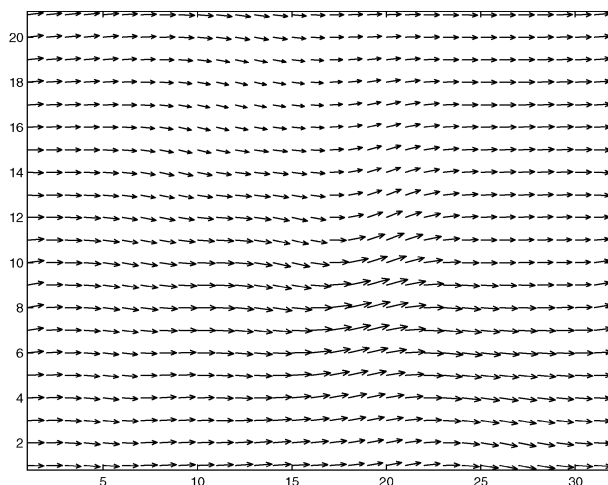


FIG. 3. Analysis based on the observations shown in Fig. 2.

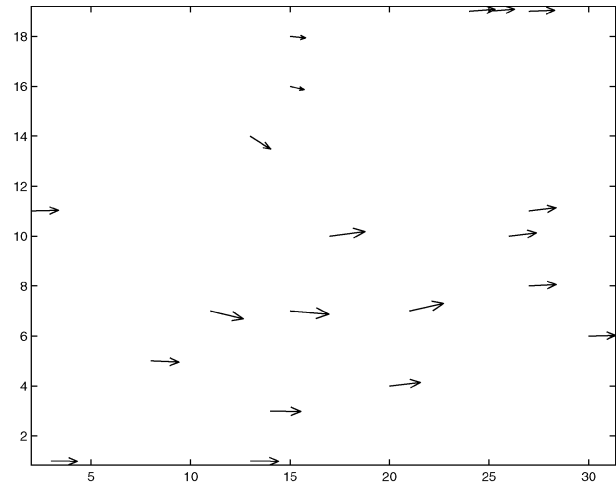


FIG. 4. Orthogonal LOS observations of the state as shown in Fig. 1.

is largest for the  $u$  component because the projection of this component on the particular LOS shown in Fig. 2 is the larger of the two.

In Fig. 4, a random set of dual-perspective observations is shown for  $p = 40$  and LOS azimuth angles (defined as the positive angle between the local meridian and the line of sight) of  $60^\circ$  and  $150^\circ$  (note that  $p = 40$  translates into 20 complete vector observations). An analysis obtained from the observations in Fig. 4 is shown in Fig. 5. The analysis is based on the same background wind error covariance formulation as the one used for the single-perspective analysis in Fig. 3. It is clear that the dual-perspective analysis is superior to the single-perspective analysis for the flow configuration and the parameters shown here. The analyzed eddy has the correct location and horizontal extent, with the main shortcoming being a lack in intensity. The rms analysis error with respect to the background field is now  $0.8$  and  $1.3 \text{ m s}^{-1}$  for  $u$  and  $v$ , respectively, which

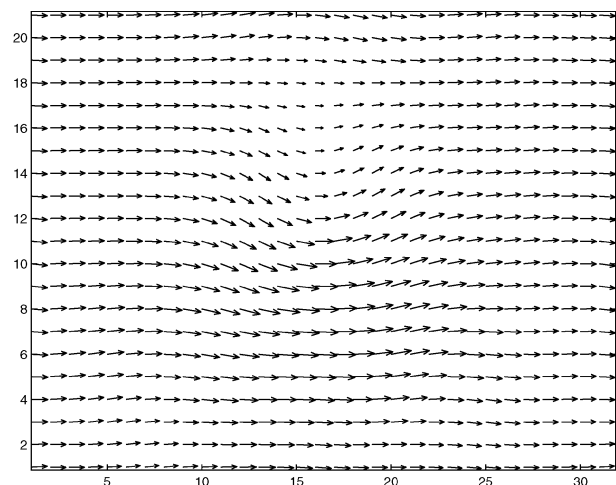


FIG. 5. Analysis based on the observations shown in Fig. 4.

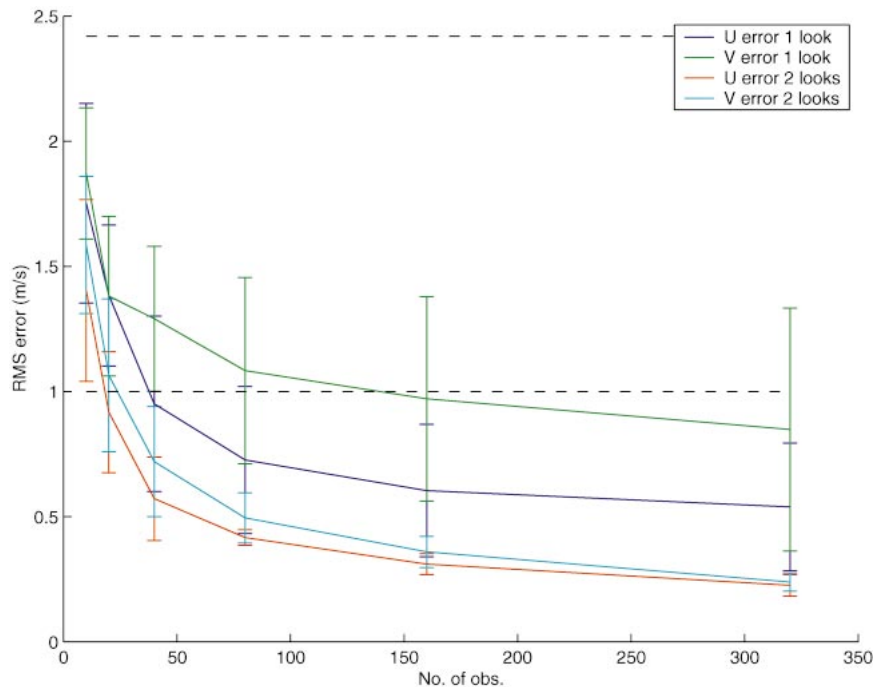


FIG. 6. Analysis errors for  $u$  and  $v$  for one and two perspectives vs the number of observations  $p$ . The solid lines show the mean error over 15 independent experiments for each value of  $p$ , and the error bars show the standard deviation of the errors. Note that, although the number of LOS (number of observations) is the same for one vs two perspectives, the number of sounding locations for the two-perspective case is one-half of that for the one-perspective case. The dashed line at  $2.4 \text{ m s}^{-1}$  denotes the rms variability in the true wind field (Fig. 1); the dashed line at  $1 \text{ m s}^{-1}$  denotes the random error in the wind component observations.

again indicates a substantial improvement over what was seen in the single-perspective analysis.

To examine the difference between the one-versus two-perspective analyses more extensively, a series of experiments similar to the ones just described was carried out with values of  $p$  ranging from 10 to 320. For each value of  $p$ , 15 single-perspective and 15 dual-perspective experiments were carried out to generate reasonably robust statistics. In each individual single-perspective experiment, the azimuth LOS angle was randomly selected between  $0^\circ$  and  $180^\circ$ . The purpose of this approach was to obtain a representative sample of experimental results irrespective of any preferential direction present in the truth and/or background states.

In Fig. 6, the mean and standard deviations of the rms analysis errors for  $u$  and  $v$  are shown for both single- and dual-perspective experiments as functions of  $p$ . Again, it is clear that the analyses based on dual-perspective observations are superior to the ones based on the single LOS winds. The difference between the two increases with  $p$ , indicating that true vector information gets increasingly important at smaller scales, whereas the impact of the scalar single-perspective observations saturates at a relatively coarse resolution (low number) of observations. The analysis error of the dual-perspective experiments is also more robust: lower error bars in the plot indicate relatively uniform analysis errors

over the 15 experiment samples. This result is probably mostly due to the fact that the impact of the single LOS observations on a given wind component is sensitive to the alignment between the individual LOS and that component.

Note that the analysis error for the dual-perspective experiments saturates at around  $0.25 \text{ m s}^{-1}$ , well below both observation and background errors. This result is consistent with what one would expect from estimation theory, assuming that the error covariances are correctly specified. The analysis error for the single-perspective experiments, on the other hand, saturates at levels that are 3–4 times as large. This supports the notion discussed in the previous section that even the simple non-divergent flow configuration tested here cannot be fully determined from observations along a single direction, even though it only contains one degree of freedom per grid point.

#### *b. Coincident versus separately located dual-perspective observations*

In the previous section it was shown that dual-perspective observations are much more useful than single-perspective observations for reducing the analysis error in the simple test case explored here. One of the issues that would need to be addressed before one can specify

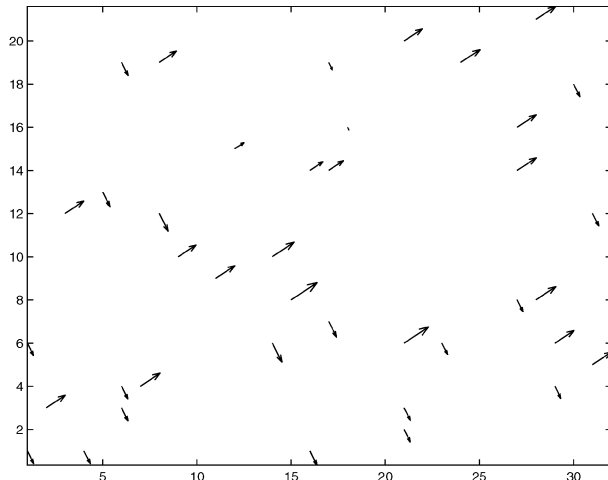


FIG. 7. An example of orthogonal LOS observations at separate horizontal locations of the state shown in Fig. 1.

the user requirements for dual-perspective observations is the level of spatial and temporal coincidence that would be required between the two perspectives. It is likely that a somewhat relaxed requirement on this will provide added degrees of freedom in the design and/or the operations phase of a given instrument. We do not explore here the issue of temporal coincidence beyond simply noting that if the two perspectives of a given atmospheric situation are obtained during one overflight (same orbit), the time difference between them would at most be on the order of minutes. This is insignificant

when compared with the temporal resolution of the analyses and of the rest of the observing system.

To test the performance of observations in the limit of an extremely low degree of spatial coincidence, a series of experiments was carried out with observations taken along two orthogonal directions but at random, separate locations. The overall flow is thus sampled along two independent directions, but any individual location is likely to be sampled along just one of these directions. An example of such observations for  $p = 40$  is shown in Fig. 7.

Again, the total number of observations  $p$  was allowed to vary, and, for each  $p$ , 15 individual experiments were carried out. The resulting analysis errors with uncertainty estimates are shown in Fig. 8 as functions of  $p$  (see Fig. 6 caption). Even though the collocated-perspectives experiments tend to outperform the separate-perspectives experiments in the middle range of  $p$  values, the two sets of curves are much closer together for all values of  $p$  than is seen in Fig. 6. The two sets of experiments are similar also in their level of consistency over the 15 experiment samples (roughly similar error bars). Overall, the results indicate that, from an analysis point of view, getting independent information about the two wind components is of paramount importance, whereas it seems to be considerably less important that these two pieces of information be obtained at the exact same geographical locations. In particular, we note that, for the single-perspective observations, the analysis error saturates at the  $0.7 \text{ m s}^{-1}$  level (Fig. 6), with no apparent benefit to be expected

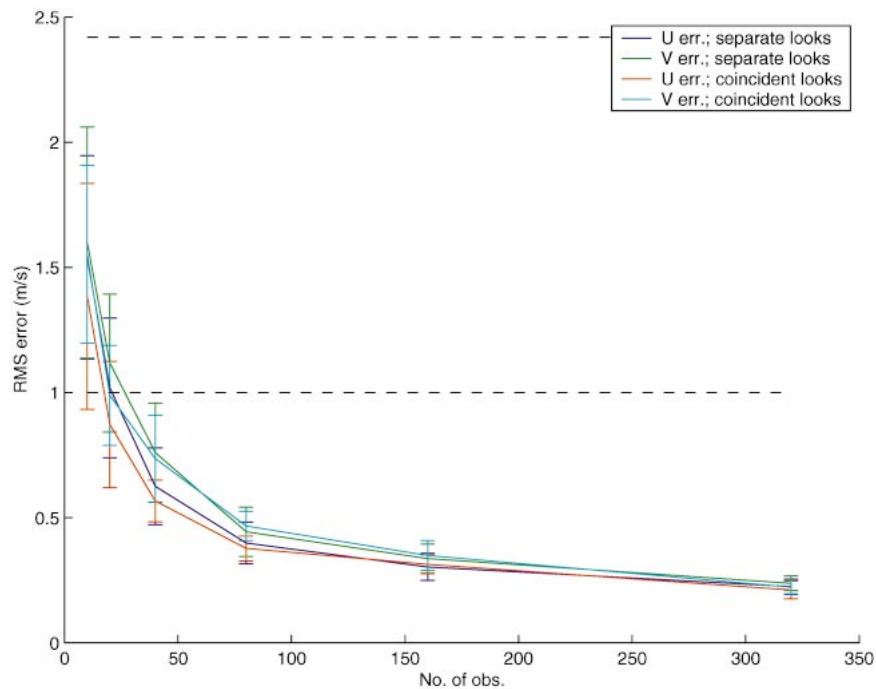


FIG. 8. Mean analysis errors with error bars, similar to Fig. 6, but for two orthogonal perspectives obtained at either separate or coincident locations.

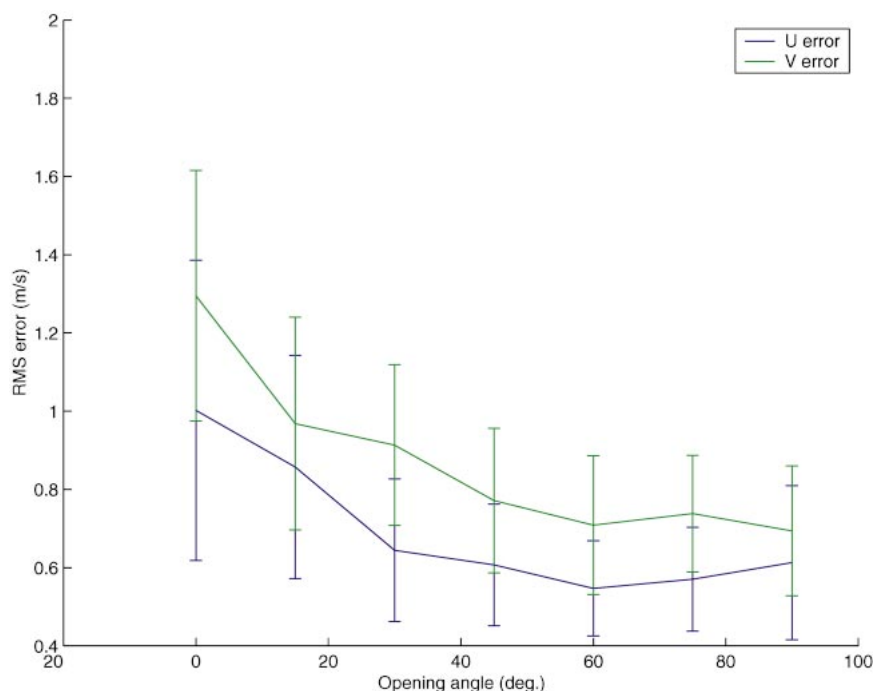


FIG. 9. Mean  $u$  and  $v$  analysis errors with error bars for dual-perspective observations,  $p = 50$ , as a function of the angle between the two wind observations.

from increasing the number of observations beyond the maximum value of 320. In the dual-perspective, separate location experiments shown in Fig. 8, the mean analysis error has fallen well below  $0.7 \text{ m s}^{-1}$  already at  $p = 80$  (40 observation pairs).

### c. Angle between perspectives

The experiments described thus far were all based on either orthogonal or parallel perspectives. The evidence is that there are substantial benefits to be harvested from obtaining orthogonal perspectives. Some proposed instrument configurations fall in between these two extremes in providing two perspectives along intersecting but nonorthogonal lines of sight. It is, therefore, of interest to study also the impact of dual-perspective observations as a function of the angle between the lines of sight.

In Fig. 9, the mean analysis error and uncertainty are shown for a series of experiments in which the angle  $\alpha$  between the two lines of sight was varied from  $0^\circ$  to  $90^\circ$ . The total number of observations was held fixed at  $p = 50$  for these experiments. For each value of  $\alpha$ , 15 experiments were run, and the overall orientation in space of the two LOS was selected randomly for each experiment in order to generate reliable statistics for both wind components. It is seen that the analysis skill improves dramatically when  $\alpha$  increases from  $0^\circ$  to  $30^\circ$ . From  $30^\circ$  to  $60^\circ$  there is a modest improvement, and beyond  $60^\circ$  the analysis error is nearly constant.

### d. Impact of the covariance model

As already mentioned, both the truth and background fields used in our experiments are nondivergent. All experiments discussed so far in the paper have been based on a forecast error covariance model that assumes nondivergence of the error. This ensures that the analysis increment, and therefore the analysis itself, will be nondivergent. For real applications, one would typically assume a mix of divergent and nondivergent errors, and at any given location the real error is likely to be of a different composition than the average mix of the two that is assumed in the covariance model. It is, therefore, of interest to see how the conclusions presented so far would be affected by using a more realistic background error covariance model.

To test this question, a series of experiments was carried out using the same nondivergent truth and background states as for the previous experiments but a background error covariance that assumed a mix of divergent and nondivergent errors.

Using the basic fact that a divergent (fully irrotational) velocity field can be derived from a velocity potential  $\chi$  (Helmholtz theorem; e.g., Holton 1992),

$$\mathbf{u} = -\nabla\chi, \quad (8)$$

and using an argument entirely parallel to Eqs. (4)–(7), we see that the error covariance of a divergent wind field can be derived from the error covariance of an underlying velocity potential:



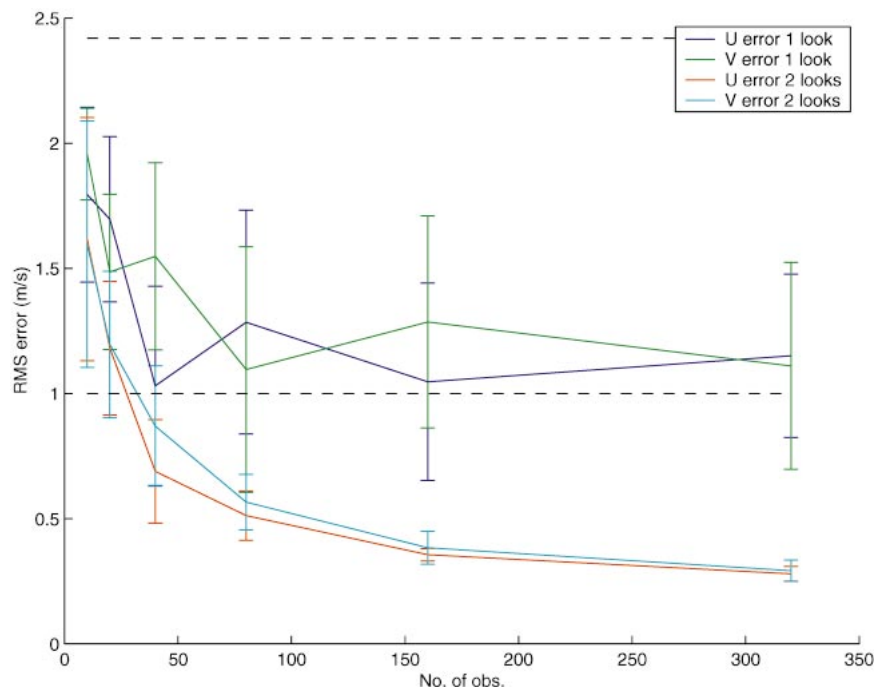


FIG. 10. Mean  $u$  and  $v$  analysis errors with error bars, similar to Fig. 6, but for a mixed rotational/divergent forecast error covariance model.

$$\mathbf{P}_u^b = \mathbf{B}\mathbf{P}_\chi^b\mathbf{B}^T, \quad (9)$$

where  $\mathbf{B}$  is the operator used for obtaining the gradient of the velocity potential in the discretized version of Eq. (8). Under the reasonable assumption that the rotational and divergent components of the wind error are mutually uncorrelated, the total wind error covariance is simply the sum of the error covariances from Eqs. (7) and (9). In our experiments, the relative error variances of the streamfunction and velocity potential were set so that the magnitude of the rotational increment was 4 times that of the divergent increment. Because the actual wind error is fully rotational, this amounts to a misspecification of the error characteristics. To expect a full recovery from the background error with such an error specification effectively constitutes a severe test of the resolution of the observing system. It is nonetheless relevant to test the extent to which various observing geometries and configurations can provide information about the divergence characteristics of the flow that is truly independent from any assumptions about the background error.

Figure 10 shows a summary plot similar to the one shown in Fig. 6, except that it is now assumed that the forecast error contains both a rotational and a divergent component as described in the two previous paragraphs.

For the experiments with two separate perspectives, the error saturates at close to the same level as that of Fig. 6. However, for the single-perspective experiments, the error apparently is saturating already at a fairly low number of observations (40). Furthermore, the error lev-

el of saturation is above the level of the background error ( $1 \text{ m s}^{-1}$ , indicated by the lower of the two dashed lines in the plot). This result is consistent from what one would expect from a misspecified background error covariance. These results indicate that a single-perspective system would put much more of a burden on the assimilation system in terms of correctly discerning even basic characteristics of the flow and that the quality of the outcome would be much more sensitive to the specification of the background error. Dual-perspective observations, on the other hand, can provide the analysis system with the means to overcome even a fairly drastic misspecification of the background error. Of interest is that they can also continue to improve the analysis result at very high resolutions, even in a case such as the one studied here in which the background error is of a relatively large scale.

#### e. Observation error versus coverage

For an active instrument such as a DWL, there is a trade-off to be made between the number of observations that can be provided per time interval and the accuracy of these observations, essentially because an increased level of accuracy requires a larger number of raw measurements per final “observation” or retrieved parameter. The designed energy consumption of the laser sets a limit to the maximum number of measurements that can be obtained per time unit, and there is, therefore, a trade-off between the total number of retrievals and

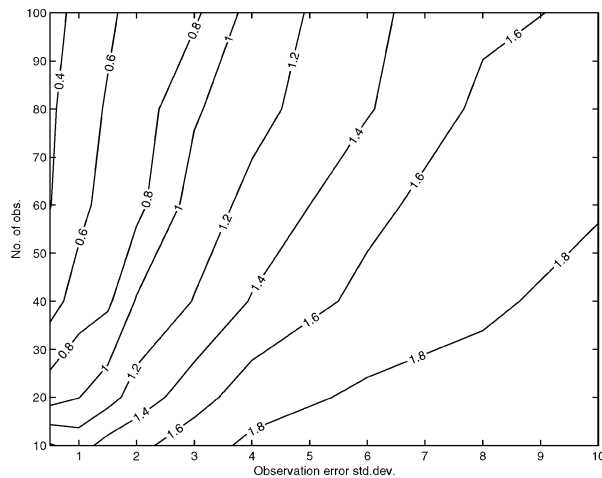


FIG. 11. The  $u$  component analysis errors (noted on contours) as a function of various combinations of individual observation error (abscissa) and the number of observations (ordinate). Dual-perspective sampling is assumed.

their individual accuracy. A set of experiments in which the number of observations and the observation error standard deviation were varied simultaneously was set up to illustrate how this trade-off can be seen from the point of view of the analysis.

Truth and background states were the same as for the experiments described so far in this article, and the background error was specified (correctly) to be fully rotational. Only dual-perspective experiments were done, and the total number of observations was allowed to vary from  $p = 10$  to  $p = 100$ . For each value of  $p$ , the observations were simulated—and subsequently fed into the analysis—with error standard deviations ranging from  $\sigma_o = 1 \text{ m s}^{-1}$  to  $\sigma_o = 10 \text{ m s}^{-1}$ . For each ( $p$ ,  $\sigma_o$ ) pair, 15 experiments were run, and the rms analysis error for  $u$  and  $v$  was calculated for each of these experiments.

Figure 11 shows the rms analysis error for the  $u$  component as a function of  $\sigma_o$ , the observation error (abscissa), and  $p$ , the total number of observations (ordinate). Each point in the plot corresponds to the mean over the 15 experiments carried out for that particular combination of  $p$  and  $\sigma_o$ .

It is immediately evident from Fig. 11 that there is a close connection between the number of observations and the observation error and the analysis error. It is also evident that even very large random observation errors can still lead to a useful analysis, in particular, when there is an abundance of observations. The reader is discouraged from dwelling too much on particular numbers given here. The observations are simulated to be unbiased and have mutually uncorrelated random errors. Neither of these assumptions would probably hold for a real instrument, and the potential impact of high observation errors is therefore likely to be overestimated in our experiments. However, it remains true that ob-

servations with errors of the same magnitude, or even larger, than the background error are likely to have an impact if there are a large number of them.

As mentioned earlier in this article, from a numerical weather prediction and data assimilation point of view, the purpose of bringing in an observation is to reduce the error of the initial condition of the forecast model, that is, to minimize the analysis error. A reasonable end-user requirement for a given observing system targeted at NWP applications could well be formulated in terms of acceptable analysis error. Again without regard for the actual numbers, the plot in Fig. 11 is a clear illustration of the fact that even a very specific goal in terms of acceptable analysis error can be achieved via a number of different routes in terms of quality versus quantity of the observations.

#### 4. Discussion

The results shown in the previous section provide a fairly strong indication that it would be preferable to obtain LOS wind observations along two independent directions rather than along one. It is admitted that the analysis system, the simulated observations, and the flow configurations studied here are gross simplifications of the corresponding real-world systems, and one might therefore be concerned whether the findings on one versus two perspectives do indeed carry over to real NWP applications and real observing systems. It is worth emphasizing again that most of the experiments described here actually tend to favor the single-perspective experiments. The basic test to which the observations are subjected is to help the analysis recover from a nondivergent error that is correctly specified, in the sense that it uses a background error covariance matrix that is derived under the assumption of nondivergence. This test is much easier to pass than is the more realistic one of correcting an error with an unknown mix of rotational and divergent components to which real-world analysis systems are subjected. An incomplete observing system, such as a single-perspective wind instrument, will thus get a substantial amount of help from the correctly specified background error covariance matrix in our experiments, whereas a real-world observing system would have to overcome not only an erroneous background field but also an incorrectly specified background error covariance.

Providing only single-component wind observations thus puts a large part of the burden of getting a correct analysis on the first guess and on the assumptions underlying the error covariance model. This approach is likely to work well whenever the background field is reasonable and the balance assumptions built into the covariance matrix are valid. However, if the purpose of flying a satellite DWL is specifically to reduce the frequency of abnormally large forecast errors, it is clear that the observations would be particularly valuable when and where new and unexpected developments oc-

cur, that is, precisely in those situations in which the background field, by definition, is in error. One might fear that these situations could also be ones in which the normal assumptions about geostrophy and, hence, nondivergence could be violated.

## 5. Summary and conclusions

The question of information content in wind observations obtained along one versus two directions has been examined in the context of a simple analysis system. Information content is defined here as the ability to reduce the analysis error. It was shown that dual-perspective observations are more than 2 times as efficient in reducing analysis errors as compared with an equal number of single-perspective measurements. It was further shown that the two perspectives need not be strictly collocated, as long as the flow field is sampled sufficiently along two independent directions. Nor do the two perspectives need to be exactly orthogonal. Most of the benefits from having dual perspectives are realized when the angle between the lines of sight is larger than  $60^\circ$ . The quality of the analysis decreases with the angle when this is less than  $30^\circ$ .

The impact of an incorrect (but realistic) specification of the background error covariance was illustrated through a series of experiments in which a rotational background error was imposed but the observations were assimilated with a mixed rotational/divergent background error covariance matrix. Results from these experiments showed that biperspective observations allowed for the analysis system to capture correctly the rotational true state, whereas the impact of the single-perspective observations saturated at a relatively low number of observations and at a substantially higher level of analysis error.

In the final series of experiments presented, the total observation error and the total number of observations were varied simultaneously to illustrate that there is no unique combination of these two parameters that will lead to a certain desired analysis accuracy. This outcome provides instrument designers with additional degrees of freedom within an overall target specified in terms of analysis accuracy.

For the application of these findings to real observing systems, it was argued that the results may tend to be too positive toward the single LOS observations. It is, therefore, likely that the difference between analyses of single-versus dual-perspective wind observations would

be even larger in a more complete analysis system, especially as analysis systems continue to move toward higher and higher horizontal resolution. Some of these issues will be addressed through future work planned to be done with the simple two-dimensional analysis system. This work will be based on real meteorological situations, and the observations will be simulated using realistic satellite data acquisition patterns.

*Acknowledgments.* The authors thank Ron Ticker of NASA Headquarters for providing support for these experiments. The first author also thanks Steve Cohn of the Data Assimilation Office for sharing his insights and experience in wind error covariance modeling.

## REFERENCES

- Atlas, R. A., 1997: Atmospheric observations and experiments to assess their usefulness in data assimilation. *J. Meteor. Soc. Japan*, **75**, 111–130.
- Cohn, S. E., A. da Silva, J. Guo, M. Sienkiewicz, and D. Lamich, 1998: Assessing the effects of data selection with the DAO Physical-Space Statistical Analysis System. *Mon. Wea. Rev.*, **126**, 2913–2926.
- Emmitt, G. D., 1987: Error analysis for total wind vector computations using one component measurements from a space-based Doppler lidar. *Proc. Optical Society of America's Fourth Conference on Coherent Laser Radar: Technology and Applications*, Aspen, CO, Optical Society of America, 217–220.
- European Space Agency, 1999: Atmospheric dynamics mission. ESA Rep. SP-1233, 157 pp.
- Gentry, B., C. L. Korb, R. Atlas, and S. Li, 1998: Zephyr: A direct detection Doppler lidar global wind sensing mission. *Optical Society of America's Annual Meeting*, Baltimore, MD, Optical Society of America, 157–158.
- Holton, J. R., 1992: *An Introduction to Dynamic Meteorology*. 3d ed. Academic Press, 511 pp.
- Lönnerberg, P., and A. Hollingsworth, 1986: The statistical structure of short-range forecast errors as determined from radiosonde data. Part II: The covariance of wind and height errors. *Tellus*, **38A**, 137–161.
- Lorenc, A., 1986: Analysis methods for numerical weather prediction. *Quart. J. Roy. Meteor. Soc.*, **112**, 205–240.
- Menzel, W. P., 2001: Cloud tracking with satellite imagery: From the pioneering work of Ted Fujita to the present. *Bull. Amer. Meteor. Soc.*, **82**, 33–47.
- Riishøjgaard, L. P., and Y. Zhu, 2002: Impact of MODIS winds on DAO systems. *Proc. Sixth Int. Winds Workshop*, Madison, WI, EUMETSAT, 263–268.
- Velden, C. S., C. M. Hayden, S. J. Nieman, W. P. Menzel, S. Wanzong, and J. S. Goerss, 1997: Upper-tropospheric winds derived from geostationary satellite water vapor observations. *Bull. Amer. Meteor. Soc.*, **78**, 173–195.
- World Meteorological Organization, 2000: *Workshop on the Impact of Observing Systems on Numerical Weather Prediction Systems*. WMO, 203 pp.